



Accurate Computer Simulation Phase-Shifting Digital Interferometry for Measurement of the Optical Properties of Zamzam Water in the Visible Spectrum

Nasser A. Moustafa^{1,2}, Hasan Assaedi² and Thamer H. Albaqami²

¹Physics Department, Faculty of Science, Helwan University, Cairo, Egypt

²Department of Physics, University College in Aljumum, Umm Al-Qura University,

P.O. Box 715, Makkah 21955, Saudi Arabia

Abstract

Refractive indices of Zamzam, bottled drinking and distilled waters have been measured by computer simulation phase shifting digital interferometry at six discrete wavelengths across the visible spectrum. Some optical parameters related to the refractive index were deduced, such as: specific refraction; polarization; group refractive index; permittivity; transmittance and reflectance. The dispersion of the deduced optical parameters across the visible spectrum was calculated. The computer simulation phase shifting digital interferometer have been used to design an experimental setup to investigate the intensity distribution of the correlation fringes obtained for Zamzam, bottled drinking and distilled waters. The present computer simulation phase shifting digital interferometer and the new theoretical formulae have been confirmed with a previous experimental results. Error value of the measured and the calculated optical parameters have been given. A detailed study between the new equations and the Cauchy dispersion equation is presented. The present study proved that Zamzam water has special and distinct optical properties that are different than those of bottled drinking and distilled waters.

Keywords: Zamzam water, phase-shifting digital interferometry, optical properties, dispersion.

Introduction

The discovery of phase-shifting interferometry (PSI) was a great progress in the field of interferometry, providing a method to measure the optical phase to unprecedented precision.

By employing different algorithms for extracting a phase map from several highly intense fringe patterns [1-4], PSI has been implemented using almost all kinds of interferometric imaging systems. For all algorithms, a discrete or continuous temporal phase shift is presented. By measuring the intensity upon phase change, the phase can be obtained. The phase is shifted by a known amount between each intensity measurement, which is called phase-shifting technique. While the intensity is integrated, which is called integrating-bucket technique. A large number of phase-stepping algorithms have been proposed [5-9]. In the present work, the computer simulation applied to the phase-stepping algorithms for measurement of the optical properties of Zamzam water in the visible spectrum.

*Corresponding author: Nasser A. Moustafa, E-mail: nasseramoustafa@gmail.com, Tel.: 002011 21509002

Received: 10/08/2023; Accepted: 13/12/2023

DOI: 10.21608/EJPHYSICS.2023.225657.1090

©2023 National Information and Documentation Center (NIDOC)

Computer simulations is a great tool for studying speckle and for designing new experimental settings. Fuji [10] described the distribution of intensity and contrast of image speckle patterns of different objects for different surface features that were examined on a computer as a function of the surface roughness characteristics of the objects and the point spread of the imaging system.

A theoretical background for the experimental results obtained by Fujii and Asakura [11] can be given by the computer simulation study for the objects having a random surface. Using the Abbe refractometer, the refractive indices of Zamzam water samples are measured at six separated wavelengths across the visible spectrum [12]. Also some associated optical parameters for the refractive index have been studied, such as: group refractive index; permittivity; specific refraction; polarizability; reflectance; and transmittance. Abbe number and the single oscillator constants for the three waters have been also calculated. It was concluded that the optical properties of Zamzam water has a distinctive feature that differ than those of bottled drinking and distilled waters. Nasser A. Moustafa, Hasan Assaedi, and Thamer H. Albaqami [13] measured the refractive index of a liquid medium by a novel computer simulation speckle photography using Fourier transform. There is an examination of the intensity distribution and contrast of the image of the speckle patterns taken from Zamzam, bottled drinking and distilled waters as a function of six different wavelengths across the visible spectrum. The result of the examination is observed and analyzed using a computer simulation programs. Using computer simulations and novel theoretical formulas, and over a wide range, the uncertainty of refractive index measurements of discrete wavelengths has been extensively studied.

In the present work, we used the computer simulation phase shifting digital interferometer to design an experimental setup to investigate the intensity distribution of the correlation fringes obtained for Zamzam , bottled drinking and distilled waters. The refractive indices of waters have been measured using the computer simulation at six discrete wavelengths across the visible spectrum. Some optical parameters related to the refractive index were deduced, such as: specific refraction; polarization; group refractive index; permittivity; transmittance and reflectance. The dispersion of the deduced optical parameters across the visible spectrum was calculated.

The Abbe numbers has been calculated and compared. The present computer simulation phase shifting digital interferometer and the new theoretical formulae have been confirmed with a previous experimental results and Cauchy's dispersion relation [14]

Theoretical background

For measuring the optical properties of a liquid, it is placed between two thin glass slides, as shown in Fig.1. , which is an illustration of a computer simulation to monitor the correlation fringes in the spectral field for Zamzam ,bottled and distilled waters. Spatially coherent light travels through a system of two glass slides and the liquid between them, illuminating a rough surface. By applying a rotation and non rotation states to the incident laser beam, and by falling the transmitted beam on the rough surface, as a result there are two images on the observation plane (CDD plane), which are digitally combined [15] to give the correlation fringes.

Phase stepping algorithm

For given the phase measurement, which is required for the measurement of the refractive index of the waters. Four phase stepping algorithms were applied. The phase shift needed for automatic fringe analysis can be introduced by a piezoelectric transducer (PZT). The four phase step algorithms was used with a phase shift $\pi/2$ per exposure. The intensity distribution of the corresponding correlograms can be expressed as [13].

$$I_1 = \left(\frac{1}{\lambda z}\right)^2 F^2 \{A(\xi, \eta)\} \left(2 + 2 \cos \left(2\pi\Delta\xi\omega_x - kd_1 \frac{\theta^2}{2n_g^2} - kd_2 \frac{\theta^2}{2n_g^2 n_\ell^2} - kd_3 \frac{\theta^2}{2n_\ell^2 n_g^4} + \alpha_1 \right) \right)$$

for $\alpha_1 = 0$ (1)

$$I_2 = \left(\frac{1}{\lambda z}\right)^2 F^2 \{A(\xi, \eta)\} \left(2 + 2 \cos \left(2\pi\Delta\xi\omega_x - kd_1 \frac{\theta^2}{2n_g^2} - kd_2 \frac{\theta^2}{2n_g^2 n_\ell^2} - kd_3 \frac{\theta^2}{2n_\ell^2 n_g^4} + \alpha_2 \right) \right)$$

for $\alpha_2 = \pi/2$ (2)

$$I_3 = \left(\frac{1}{\lambda z}\right)^2 F^2 \{A(\xi, \eta)\} \left(2 + 2 \cos \left(2\pi\Delta\xi\omega_x - kd_1 \frac{\theta^2}{2n_g^2} - kd_2 \frac{\theta^2}{2n_g^2 n_\ell^2} - kd_3 \frac{\theta^2}{2n_\ell^2 n_g^4} + \alpha_3 \right) \right)$$

for $\alpha_3 = \pi$ (3)

$$I_4 = \left(\frac{1}{\lambda z}\right)^2 F^2 \{A(\xi, \eta)\} \left(2 + 2 \cos \left(2\pi\Delta\xi\omega_x - kd_1 \frac{\theta^2}{2n_g^2} - kd_2 \frac{\theta^2}{2n_g^2 n_\ell^2} - kd_3 \frac{\theta^2}{2n_\ell^2 n_g^4} + \alpha_4 \right) \right)$$

for $\alpha_4 = 3\pi/2$ (4)

The phase needed for the measurement of the refractive index n_ℓ is obtained from the intensity distributions of Eqs. (1) to (4), and is given by:

$$\Phi = \tan^{-1} \frac{I_4 - I_2}{I_1 - I_3} \quad (5)$$

Where the thicknesses of the two glass slides are d_1 and d_3 respectively, also the thickness of the liquid is d_2 . The incident plane wave continues to propagate as a plane wave with wavenumber k , and makes an angle θ with the x-axis of the system. Where n_g is the refractive index of the glass plate. The new equation of the refractive index [13] n_ℓ is related to the fringe spacing λ_x , which can be determined from the phase map of equation (5). $\omega_x = 2\pi/\lambda_x$, and $\Delta\xi = M\xi_m = \lambda z/\lambda_x$, M is the magnification of the imaging system, and ξ_m is the mechanical displacement used for the calibration of the system [15].

Optical parameters fundamentals

Refractive index

The refractive index of a medium representing by the ratio of the vacuum velocity of an electromagnetic wave to its phase velocity in the medium. The measurement of the refractive indices of different materials have been reviewed [16] by various techniques. By using the new refractive index formulae which is confirmed by the novel computer simulation speckle photography method using Fourier transform [13], the optical parameters of the different liquids can be obtained.

The refractive index is given by:

$$n_\ell = \sqrt{\frac{\theta^2 \left(d_2 + \frac{d_3}{n_g^2} \right)}{2\lambda n_g^2 \left(2\pi \frac{\lambda z}{\lambda_x^2} - \frac{d_1}{\lambda} \frac{\theta^2}{2n_g^2} - 1 \right)}} \quad (6)$$

The refractive index dispersion is its change with the wavelength and can be written as:

$$\frac{dn_\ell(\lambda)}{d\lambda} = \left(\frac{-1}{2} \right) \frac{\left(\theta^2 (d_2 + d_3/n_g^2) / 2n_g^2 \right)^{1/2} \left(4\pi\lambda z / \lambda_x^2 - 1 \right)}{\left(\frac{2\pi\lambda z}{\lambda_x^2} - \frac{d_1\theta^2}{2n_g^2} - \lambda \right)^{3/2}} \quad (7)$$

Group refractive index

The group refractive index of the medium is defined as the ratio of the vacuum velocity of the electromagnetic wave to its group in a medium. To measure the group refractive index for thin solid and liquid

materials, fringes of equal chromatic order were used [17]. From equation 7, which represent the dispersion relation of the measured values of the refractive index, the group refractive index can be calculated mathematically. And it can be written as:

$$N_g(\lambda) = n_\ell(\lambda) - \lambda \left[\frac{dn_\ell(\lambda)}{d\lambda} \right] \tag{8}$$

From equations 6 and 7 we get:

$$N_g(\lambda) = \sqrt{\frac{\theta^2 \left(d_2 + \frac{d_3}{n_g^2} \right)}{2\lambda n_g^2 \left(2\pi \frac{\lambda z}{\lambda_x^2} - \frac{d_1}{\lambda} \frac{\theta^2}{2n_g^2} - 1 \right)}} - \lambda \left(\frac{-1}{2} \right) \frac{\left(\theta^2 (d_2 + d_3 / n_g^2) / 2n_g^2 \right)^{1/2} \left(\frac{4\pi\lambda z}{\lambda_x^2} - 1 \right)}{\left(\frac{2\pi\lambda^2 z}{\lambda_x^2} - \frac{d_1\theta^2}{2n_g^2} - \lambda \right)^{3/2}} \tag{9}$$

The dispersion of the group refractive index is its change with the wavelength and can be written as:

$$\frac{dN_g(\lambda)}{d\lambda} = \left(\frac{1}{2} \right) \frac{\left(\theta^2 (d_2 + d_3 / n_g^2) / 2n_g^2 \right)^{1/2} \left(\frac{2\pi\lambda z}{\lambda_x^2} \right)}{\left(\frac{2\pi\lambda^2 z}{\lambda_x^2} - \frac{d_1\theta^2}{2n_g^2} - \lambda \right)^{3/2}} + \left(\frac{-3\lambda}{4} \right) \frac{\left(\theta^2 (d_2 + d_3 / n_g^2) / 2n_g^2 \right)^{1/2} \left(\frac{2\pi\lambda z}{\lambda_x^2} - 1 \right) \left(\frac{4\pi\lambda z}{\lambda_x^2} - 1 \right)}{\left(\frac{2\pi\lambda^2 z}{\lambda_x^2} - \frac{d_1\theta^2}{2n_g^2} - \lambda \right)^{3/2}} \tag{10}$$

Permittivity

From the Maxwell's relation [18], the permittivity of a dielectric material can be written as:

$$\epsilon(\lambda) = [n(\lambda)]^2 \tag{11}$$

From equation 5,

$$\epsilon_\ell(\lambda) = \frac{\theta^2 \left(d_2 + \frac{d_3}{n_g^2} \right)}{2\lambda n_g^2 \left(2\pi \frac{\lambda z}{\lambda_x^2} - \frac{d_1}{\lambda} \frac{\theta^2}{2n_g^2} - 1 \right)} \tag{12}$$

The dispersion of the permittivity is written as:

$$\frac{d\epsilon_\ell(\lambda)}{d\lambda} = 2n_\ell(\lambda) \frac{dn_\ell(\lambda)}{d\lambda} \tag{13}$$

From equations 6 , and 7, we get:

$$\frac{d\varepsilon_i(\lambda)}{d\lambda} = 2 \left(\frac{\theta^2 \left(d_2 + \frac{d_3}{n_g^2} \right)}{2\lambda n_g^2 \left(2\pi \frac{\lambda z}{\lambda_x^2} - \frac{d_1}{\lambda} \frac{\theta^2}{2n_g^2} - 1 \right)} \right)^{\frac{1}{2}} \left(\frac{-1}{2} \right) \frac{(\theta^2 (d_2 + d_3 / n_g^2) / 2n_g^2)^{\frac{1}{2}} (4\pi\lambda z / \lambda_x^2 - 1)}{\left(\frac{2\pi\lambda z}{\lambda_x^2} - \frac{d_1\theta^2}{2n_g^2} - \lambda \right)^{\frac{3}{2}}} \quad (14)$$

Specific Refraction

The specific refraction of a dielectric material is defined as [18]:

$$S(\lambda) = \frac{[n(\lambda)^2 - 1]}{[n(\lambda)^2 + 2]} \quad (15)$$

From equation 6,

$$S_i(\lambda) = \frac{\left(\frac{\theta^2 \left(d_2 + \frac{d_3}{n_g^2} \right)}{2\lambda n_g^2 \left(2\pi \frac{\lambda z}{\lambda_x^2} - \frac{d_1}{\lambda} \frac{\theta^2}{2n_g^2} - 1 \right)} \right) - 1}{\left(\frac{\theta^2 \left(d_2 + \frac{d_3}{n_g^2} \right)}{2\lambda n_g^2 \left(2\pi \frac{\lambda z}{\lambda_x^2} - \frac{d_1}{\lambda} \frac{\theta^2}{2n_g^2} - 1 \right)} \right) + 2} \quad (16)$$

The dispersion of the specific refraction is:

$$\frac{dS_i(\lambda)}{d\lambda} = \frac{[6n_i(\lambda)]}{[n_i(\lambda)^2 + 2]^2} \left[\frac{dn_i(\lambda)}{d\lambda} \right] \quad (17)$$

From equations 6, and 7, we get:

$$\frac{dS_i(\lambda)}{d\lambda} = \frac{\left[\left(\frac{\theta^2 \left(d_2 + \frac{d_3}{n_g^2} \right)}{2\lambda n_g^2 \left(2\pi \frac{\lambda z}{\lambda_x^2} - \frac{d_1}{\lambda} \frac{\theta^2}{2n_g^2} - 1 \right)} \right)^{\frac{1}{2}} \right]}{\left(\left(\frac{\theta^2 \left(d_2 + \frac{d_3}{n_g^2} \right)}{2\lambda n_g^2 \left(2\pi \frac{\lambda z}{\lambda_x^2} - \frac{d_1}{\lambda} \frac{\theta^2}{2n_g^2} - 1 \right)} \right) + 2 \right)^2} \left(\frac{-1}{2} \right) \frac{(\theta^2 (d_2 + d_3 / n_g^2) / 2n_g^2)^{\frac{1}{2}} (4\pi\lambda z / \lambda_x^2 - 1)}{\left(\frac{2\pi\lambda z}{\lambda_x^2} - \frac{d_1\theta^2}{2n_g^2} - \lambda \right)^{\frac{3}{2}}} \quad (18)$$

Polarizability per unit volume

The polarizability per unit volume of a dielectric material is written as [19]:

$$P(\lambda) = \frac{\left[\frac{3}{4\pi} \left[n(\lambda)^2 - 1 \right] \right]}{\left[n(\lambda)^2 + 2 \right]} \tag{19}$$

From equation 6,

$$P_\ell(\lambda) = \frac{\left(\frac{3}{4\pi} \left[\frac{\theta^2 \left(d_2 + \frac{d_3}{n_g^2} \right)}{2\lambda n_g^2 \left(2\pi \frac{\lambda z}{\lambda_x^2} - \frac{d_1}{\lambda} \frac{\theta^2}{2n_g^2} - 1 \right)} \right] - 1 \right)}{\left(\frac{\theta^2 \left(d_2 + \frac{d_3}{n_g^2} \right)}{2\lambda n_g^2 \left(2\pi \frac{\lambda z}{\lambda_x^2} - \frac{d_1}{\lambda} \frac{\theta^2}{2n_g^2} - 1 \right)} \right) + 2} \tag{20}$$

The dispersion of the polarizability per unit volume is:

$$\frac{dP_\ell(\lambda)}{d\lambda} = \frac{\left[\frac{3}{4\pi} \left[6n_\ell(\lambda) \right] \right] \left[\frac{dn_\ell(\lambda)}{d\lambda} \right]}{\left(n_\ell(\lambda)^2 + 2 \right)^2} \tag{21}$$

From equations 6 , and 7, we get:

$$\frac{dP_\ell(\lambda)}{d\lambda} = \frac{\left[\frac{3}{4\pi} \left[6 \left(\frac{\theta^2 \left(d_2 + \frac{d_3}{n_g^2} \right)}{2\lambda n_g^2 \left(2\pi \frac{\lambda z}{\lambda_x^2} - \frac{d_1}{\lambda} \frac{\theta^2}{2n_g^2} - 1 \right)} \right)^{\frac{1}{2}} \right] \right]}{\left(\left(\frac{\theta^2 \left(d_2 + \frac{d_3}{n_g^2} \right)}{2\lambda n_g^2 \left(2\pi \frac{\lambda z}{\lambda_x^2} - \frac{d_1}{\lambda} \frac{\theta^2}{2n_g^2} - 1 \right)} \right) + 2 \right)^2} \left(\frac{-1}{2} \right) \frac{\left(\theta^2 \left(d_2 + \frac{d_3}{n_g^2} \right) / 2n_g^2 \right)^{\frac{1}{2}} \left(4\pi \lambda z / \lambda_x^2 - 1 \right)}{\left(\frac{2\pi \lambda z}{\lambda_x^2} - \frac{d_1}{2n_g^2} - \lambda \right)^{\frac{3}{2}}} \tag{22}$$

Reflectance

In case of normal incidence, the reflectance from an air/medium interface can be written as in the following form [19]:

$$R(\lambda) = \left\{ \frac{\left[n(\lambda) - 1 \right]}{\left[n(\lambda) + 1 \right]} \right\}^2 \tag{23}$$

From equation 6,

$$R_\ell(\lambda) = \left[\frac{\left(\frac{\theta^2 \left(d_2 + \frac{d_3}{n_g^2} \right)}{2\lambda n_g^2 \left(2\pi \frac{\lambda z}{\lambda_x^2} - \frac{d_1}{\lambda} \frac{\theta^2}{2n_g^2} - 1 \right)} \right)^{1/2}}{\left(\frac{\theta^2 \left(d_2 + \frac{d_3}{n_g^2} \right)}{2\lambda n_g^2 \left(2\pi \frac{\lambda z}{\lambda_x^2} - \frac{d_1}{\lambda} \frac{\theta^2}{2n_g^2} - 1 \right)} \right)^{1/2}} - 1 \right]^2 \quad (24)$$

The dispersion of the reflectance is:

$$\frac{dR_\ell(\lambda)}{d\lambda} = \frac{[4n_\ell(\lambda)(n_\ell(\lambda) - 1)] \left[\frac{dn_\ell(\lambda)}{d\lambda} \right]}{(n_\ell(\lambda) + 1)^3} \quad (25)$$

From equations 6, and 7, we get:

$$\frac{dR_\ell(\lambda)}{d\lambda} = \frac{4 \left(\frac{\theta^2 \left(d_2 + \frac{d_3}{n_g^2} \right)}{2\lambda n_g^2 \left(2\pi \frac{\lambda z}{\lambda_x^2} - \frac{d_1}{\lambda} \frac{\theta^2}{2n_g^2} - 1 \right)} \right)^{1/2} \left(\frac{\theta^2 \left(d_2 + \frac{d_3}{n_g^2} \right)}{2\lambda n_g^2 \left(2\pi \frac{\lambda z}{\lambda_x^2} - \frac{d_1}{\lambda} \frac{\theta^2}{2n_g^2} - 1 \right)} \right)^{1/2} - 1}{\left(\frac{\theta^2 \left(d_2 + \frac{d_3}{n_g^2} \right)}{2\lambda n_g^2 \left(2\pi \frac{\lambda z}{\lambda_x^2} - \frac{d_1}{\lambda} \frac{\theta^2}{2n_g^2} - 1 \right)} \right)^{1/2} + 1} \left(\frac{-1}{2} \right) \frac{(\theta^2 (d_2 + d_3/n_g^2)/2n_g^2)^{1/2} (4\pi\lambda z/\lambda_x^2 - 1)}{\left(\frac{2\pi\lambda z}{\lambda_x^2} - \frac{d_1\theta^2}{2n_g^2} - \lambda \right)^{3/2}} \quad (26)$$

Transmittance

In case of normal incidence, the material transmittance through air/medium interface can be written as in the following form [20]:

$$T(\lambda) = \frac{4n(\lambda)}{[n(\lambda) + 1]^2} \quad (27)$$

From equation 6,

$$T_\ell(\lambda) = \frac{4 \left(\frac{\theta^2 \left(d_2 + \frac{d_3}{n_g^2} \right)}{2\lambda n_g^2 \left(2\pi \frac{\lambda z}{\lambda_x^2} - \frac{d_1}{\lambda} \frac{\theta^2}{2n_g^2} - 1 \right)} \right)^{\frac{1}{2}}}{\left[\left(\frac{\theta^2 \left(d_2 + \frac{d_3}{n_g^2} \right)}{2\lambda n_g^2 \left(2\pi \frac{\lambda z}{\lambda_x^2} - \frac{d_1}{\lambda} \frac{\theta^2}{2n_g^2} - 1 \right)} \right)^{\frac{1}{2}} + 1 \right]^2} \tag{28}$$

The dispersion of the transmittance is:

$$\frac{dT_\ell(\lambda)}{d\lambda} = \frac{[4n_\ell(\lambda) - 1]}{(n_\ell(\lambda) + 1)^3} \left[\frac{dn_\ell(\lambda)}{d\lambda} \right] \tag{29}$$

From equations 6 , and 7, we get:

$$\frac{dT_\ell(\lambda)}{d\lambda} = \frac{\left[4n \left(\frac{\theta^2 \left(d_2 + \frac{d_3}{n_g^2} \right)}{2\lambda n_g^2 \left(2\pi \frac{\lambda z}{\lambda_x^2} - \frac{d_1}{\lambda} \frac{\theta^2}{2n_g^2} - 1 \right)} \right) - 1 \right]}{\left(\left(\frac{\theta^2 \left(d_2 + \frac{d_3}{n_g^2} \right)}{2\lambda n_g^2 \left(2\pi \frac{\lambda z}{\lambda_x^2} - \frac{d_1}{\lambda} \frac{\theta^2}{2n_g^2} - 1 \right)} \right) + 1 \right)^3} \left(\frac{-1}{2} \right) \frac{\left(\theta^2 \left(d_2 + \frac{d_3}{n_g^2} \right) / 2n_g^2 \right)^{\frac{1}{2}} \left(4\pi\lambda z / \lambda_x^2 - 1 \right)}{\left(\frac{2\pi\lambda z}{\lambda_x^2} - \frac{d_1\theta^2}{2n_g^2} - \lambda \right)^{\frac{3}{2}}} \tag{30}$$

Abbe Number

The Abbe number is defined as [21] :

$$v = (n_d - 1) / (n_f - n_c) \tag{31}$$

From equation 6,

$$v_\ell = \frac{\left(\left(\frac{\theta^2 \left(d_2 + \frac{d_3}{n_g^2} \right)}{2\lambda_{\ell 1} n_g^2 \left(2\pi \frac{\lambda_{\ell 1} z}{\lambda_x^2} - \frac{d_1}{\lambda_{\ell 1}} \frac{\theta^2}{2n_g^2} - 1 \right)} \right)^{\frac{1}{2}} - 1 \right)}{\left(\left(\frac{\theta^2 \left(d_2 + \frac{d_3}{n_g^2} \right)}{2\lambda_{\ell 2} n_g^2 \left(2\pi \frac{\lambda_{\ell 2} z}{\lambda_x^2} - \frac{d_1}{\lambda_{\ell 2}} \frac{\theta^2}{2n_g^2} - 1 \right)} \right)^{\frac{1}{2}} - \left(\frac{\theta^2 \left(d_2 + \frac{d_3}{n_g^2} \right)}{2\lambda_{\ell 3} n_g^2 \left(2\pi \frac{\lambda_{\ell 3} z}{\lambda_x^2} - \frac{d_1}{\lambda_{\ell 3}} \frac{\theta^2}{2n_g^2} - 1 \right)} \right)^{\frac{1}{2}} \right)} \quad (32)$$

where n_d , n_c , and n_f are refractive indices at $\lambda_{\ell 1} = 587.56 \text{ nm}$, $\lambda_{\ell 2} = 656.27 \text{ nm}$, and $\lambda_{\ell 3} = 486.13 \text{ nm}$ respectively. It indicates approximately the dispersion of the medium across the visible spectrum.

Computer Simulation Results and Discussions

Fig.1. shows the optical setup which has been simulated by computer to monitor the correlation fringes in the spectral field for Zamzam, bottled and distilled waters. Optical configuration elucidation was implemented to introduce computer simulation phase-shifting digital interferometry as a new technique for an accurate measurement of the optical properties of Zamzam, bottled drinking and distilled waters in the visible spectrum.

A coherent laser beam of low-power laser diodes with different wavelengths across the visible spectrum ($\lambda = 632.8 \text{ nm}$, 589.3 nm , 577.0 nm , 546.1 nm , 435.8 nm , and 404.7 nm respectively) illuminated the system which consisting of two glass slides and the liquid in between. The thicknesses of the two glass slides are $d_1 = 300 \mu\text{m}$ and $d_3 = 300 \mu\text{m}$ respectively, also the thickness of the liquid is $d_2 = 250 \mu\text{m}$.

A rough surface illuminated by a spatially coherent light which transmitted through the glass plates and the liquid. The laser beam spot was kept in the diffuser plane with a diameter of 2 cm to ensure suitable speckle size. The rough surface and the imaging plane had $Z = 75 \text{ cm}$ between them. By applying a rotation and non rotation to the incident laser beam, and by falling the transmitted beam on the rough surface, as a result there are two images on the observation plane (CDD plane), which are digitally combined to give the correlation fringes.

This step is repeated four times by applying a phase shift $\frac{\pi}{2}$ in every case by moving the mirror attached to the piezoelectric transducer (PZT). From the four intensities distributions mentioned in equations, from (1) to (4), we can get the phase change on the speckle resulting from the rough surface. The average value of the phase change is calculated at a value of $3.998 \times 2\pi$.

The following figures 2,3,4,5,6,7, and 8 show the relations between the six discrete wavelengths across the visible spectrum and the refractive index $n_\ell(\lambda)$, group refractive index $N_\ell(\lambda)$, permittivity $\varepsilon_\ell(\lambda)$, polarizability $P_\ell(\lambda)$, specific refraction $S_\ell(\lambda)$, specific reflectance $R_\ell(\lambda)$, and the transmittance $T_\ell(\lambda)$ respectively. As shown in the mentioned figures, there is a comparative study of these optical properties in case of applying the new deduced theoretical equations and the Cauchy's dispersion equation for Zamzam, bottled drinking and distilled waters. From the comparative study we can observe pretty much agreement between the new equations and Cauchy's dispersion equation. Figure 9 (a,b,c,d) shows the wrapped images of the correlation fringes in the spectral field at wavelengths $0.6328 \mu m$, $0.5893 \mu m$, $0.5461 \mu m$ and $0.4047 \mu m$ respectively. The rotation angle was $\theta = 0.2^\circ$ and the distance between the rough surface and the observation plane Z was 75 cm. From these wrapped phase images, we can observe that the degree of visibility decreases as the wavelengths also decreases. The wrapped images of the correlation fringes in the spectral domain of Zamzam, bottled drinking and distilled waters can be shown in figure 10 (a,b,c) respectively. The rotation angle was $\theta = 0.2^\circ$ at wavelength $0.6328 \mu m$. The distance between the rough surface and the observation plane Z was 75 cm. From these wrapped phase images, we can observe that the degree of visibility of the correlation fringes is clearer in the case of Zamzam water than the bottled drinking and distilled waters even with a wavelength change. This explains the superiority of the visibility of the wrapped phase images in case of Zamzam water. Figure.(11) shows the relation between the six discrete wavelengths across the visible spectrum and the phase in radian Φ given by the new theoretical formulae and the phase map for Zamzam, bottled drinking and distilled waters. As we can observe from the disparity of the visibility of the wrapped phase images of the different waters. There is an effect on the measurement of the phase change on the speckle. The accuracy of measurement in case Zamzam water is more accurate than that of the other waters. There is a great compatibility between the phase in radian Φ given by the new theoretical formulae and the phase map in case of Zamzam water much more than the other waters.

Table 1. Shows the dispersion of optical parameters at $\lambda = 550nm$ for three waters using Cauchy's dispersion equation and the new theoretical equation. Dispersion values of optical parameters, at $\lambda = 550nm$, for Zamzam water are smaller than those of bottled and distilled water by 0.49 times. The Abbe number of Zamzam is 2.3 times higher than bottled water and 2.8 times higher than distilled water.

Conclusion

Computer simulation phase shifting digital interferometer have been presented for accurate measurements of the optical properties of Zamzam, bottled drinking and distilled waters. The presented method and the new theoretical formulae have been confirmed with a previous experimental results and Cauchy's dispersion relation. There is a pretty much agreement between the new equations and Cauchy's dispersion equation. The accuracy of measurement of the phase change on the speckle in case Zamzam water is more accurate than that of the other waters. There is a great compatibility between the phase in radian Φ given by the new theoretical formulae and the phase map in case of Zamzam water much more than the other waters. The uses of laser light of wavelength $0.6328 \mu m$ and with a small angle of incidence $\theta = 0.2^\circ$, give more accurate measurement of the phase change. Summary of saying that Zamzam water has special and distinct optical properties that are different than those of bottled drinking and distilled waters.

Acknowledgement

This work is funded by grant number (12-NAN2287-10) from National Science Technology and Innovation Plan (NSTP), the King Abdul-Aziz City for Science and Technology (MAARIFH), Kingdom of Saudi Arabia.

References

- 1- Joenathan, C. "Phase-measuring interferometry: new methods and error analysis," *Applied Optics*, Vol.33, Issue 19, pp.4147-4155 (1994). <https://doi.org/10.1364/AO.33.004147>
- 2- Schwider, J. "Advanced evaluation techniques in interferometry," in *Progress in Optics*, E. Wolf, ed.(Elsevier Science, New York,1990),Vol. 28, pp. 271–359.
[doi.10.1016/S0079-6638\(08\)70291-9](https://doi.org/10.1016/S0079-6638(08)70291-9)
- 3- Vikram, C. S., Witherow, W. K. and Trolinger, J. D. "Algorithm for phase-difference measurement in phase-shifting interferometry," *Applied Optics*, Vol.32, Issue 31, pp.6250-6252 (1993).
<https://doi.org/10.1364/AO.32.006250>
- 4- Reena Disawal, Jitendra Dhanotia, and Shashi Prakash,"Phase-shifting lateral shearing interferometry using wedge-plate and interferometric grating," *Applied Optics*, Vol.53, pp.7534-7539 (2014).
<https://doi.org/10.1364/AO.53.007534>
- 5- Phillion, D. W. "General methods for generating phase shifting interferometry algorithms," *Appl. Opt.* **36**, 8098– 8115 (1997). <https://doi.org/10.1364/AO.36.008098>
- 6- Hariharan, P., Oreb, B. F. and Eiju, T. "Digital phase shifting interferometry: a simple error-compensating phase calculating algorithm," *Appl. Opt.* **26**, 2504–2506 (1987). <https://doi.org/10.1364/AO.26.002504>
- 7- Larkin, K. G. and Oreb, B. F. "Design and assessment of symmetrical phase-shifting algorithms," *J. Opt. Soc. Am. A* **9**, 1740–1748 (1992). <https://doi.org/10.1364/JOSAA.9.001740>
- 8- Surrel, Y. "Phase stepping: a new self-calibrating algorithm," *Appl. Opt.* **39**, 3598–3600 (1993).
<https://doi.org/10.1364/AO.32.003598>
- 9- Schwider, J., Falkenstorfer, O., Schreiber, H., Zoller, A. and Streibl, N. "New compensating four-phase algorithm for phase-shift interferometry," *Opt. Eng.* **32**, 1883–1885(1993).
<https://doi.org/10.1117/12.143340>
- 10- Fujii, H., Uozumi, J. and Asakura, T. "Computer simulation study of image speckle patterns with relation to object surface profile", *Journal of the Optical Society of America*, Vol. 66, Issue 11, pp. 1222-1236 (1976); [doi:10.1364/JOSA.66.001222](https://doi.org/10.1364/JOSA.66.001222)
- 11- Fujii, H. J., Asaku, T. and Shindo, Y. "Measurement of surface roughness properties by using image speckle contrast" *Journal of the Optical Society of America*, Vol. 66, Issue 11, pp. 1217-1222 (1976), [doi:10.1364/JOSA.66.001217](https://doi.org/10.1364/JOSA.66.001217)

- 12- El-Zaiat, S. Y. "Group Refractive Index Measurement by Fringes of Equal Chromatic Order", *Opt. and Lasers Technol.*, **37** (2005), p. 181. <https://doi.org/10.1364/AO.48.004430>
- 13- Nasser A. Moustafa, Hasan Assaedi, and Thamer H. Albaqami "Comparative study of Zamzam, bottled drinking and distilled waters by a novel computer simulation speckle photography method using Fourier transform", *Open Journal of Applied Sciences*, **12**, 1577-1594 (2022). <https://doi.org/10.4236/ojapps.2022.129107>
- 14- Smith, D., Inokuti, M. and Karstens, W. "Cauchy's Dispersion Equation Reconsidered: Dispersion in Silicate Glasses", *Rad. Eff. and Def. in Sol.*, **157** (2002), p. 823. <https://doi.org/10.1080/10420150215781>
- 15- Nasser A. Moustafa, "Digital Processing of Speckle Photography to Measure Refractive Index of a Transparent Plate", *Australian Journal of Basic and Applied Sciences*, **7**(8), 187 -193, 2013. [doi:10.1117/12.2020374](https://doi.org/10.1117/12.2020374)
- 16- Singh, S. "Refractive Index Measurement and its Applications", *Physica Scripta*, **65** (2002), p. 167. [doi:10.1238/Physica.Regular.065a00167](https://doi.org/10.1238/Physica.Regular.065a00167).
- 17- El-Zaiat, S. Y. "Group Refractive Index Measurement by Fringes of Equal Chromatic Order", *Opt. and Lasers Technol.*, **37** (2005), p. 181. [doi:10.1016/j.optlastec.2004.03.007](https://doi.org/10.1016/j.optlastec.2004.03.007)
- 18- Catenaccio, Y. Darwich and C. Magallanes, "Temperature Dependence of the Permittivity of Water", *Chem. Phys.Lett.*, **367** (2003) p. 669. [doi:10.1016/S0009-2614\(02\)01735-9](https://doi.org/10.1016/S0009-2614(02)01735-9)
- 19- El-Kashef, H. "Optical and Electrical Properties of Materials", *Rev. Sci. Inst.*, **65** (1994) p. 2056. <https://doi.org/10.1063/1.1144812>
- 20- Pedrotti, F. and Pedrotti, L. *Introduction to Optics*. London: Prentice-Hall, 1993, p. 412. <https://doi.org/10.1017/9781108552493>
- 21- Wondraczek, L. *et al.*, "Abbe Number and Refractive Indices of Tektites and Volcanic Glasses", *J. Non-Crys. Sol.* **323**(2003) p. 127. [doi:10.1016/S0022-3093\(03\)00283-7](https://doi.org/10.1016/S0022-3093(03)00283-7)

Figure Captions

Figure (1). Illustration of computer simulation for observation of correlation fringes and phase map in the spectral field for Zamzam ,bottled drinking and distilled waters.

Figure (2). Relation between the six discrete wavelengths across the visible spectrum and the refractive index $n_\ell(\lambda)$ given by the new theoretical formulae and the Cauchy's dispersion equation for Zamzam, bottled drinking and distilled waters.

Figure.(3). Relation between the six discrete wavelengths across the visible spectrum and the group refractive index $N_\ell(\lambda)$ given by the new theoretical formulae and the Cauchy's dispersion equation for Zamzam, bottled drinking and distilled waters.

Figure.(4). Relation between the six discrete wavelengths across the visible spectrum and the permittivity $\epsilon_\ell(\lambda)$ given by the new theoretical formulae and the Cauchy's dispersion equation for Zamzam, bottled drinking and distilled waters.

Figure.(5). Relation between the six discrete wavelengths across the visible spectrum and the polarizability $P_\ell(\lambda)$ given by the new theoretical formulae and the Cauchy's dispersion equation for Zamzam, bottled drinking and distilled waters.

Figure.(6). Relation between the six discrete wavelengths across the visible spectrum and the specific refraction $S_\ell(\lambda)$ given by the new theoretical formulae and the Cauchy's dispersion equation for Zamzam, bottled drinking and distilled waters.

Figure.(7). Relation between the six discrete wavelengths across the visible spectrum and the specific reflectance $R_\ell(\lambda)$ given by the new theoretical formulae and the Cauchy's dispersion equation for Zamzam, bottled drinking and distilled waters.

Figure.(8). Relation between the six discrete wavelengths across the visible spectrum and the transmittance $T_\ell(\lambda)$ given by the new theoretical formulae and the Cauchy's dispersion equation for Zamzam, bottled drinking and distilled waters.

Figure 9 (a,b,c,d): Wrapped images of the correlation fringes in the spectral field at wavelengths $0.6328 \mu m$, $0.5893 \mu m$, $0.5461 \mu m$ and $0.4047 \mu m$ respectively. The rotation angle was $\theta = 0.2^\circ$ and the distance between the rough surface and the observation plane Z was 75 cm.

Figure 10 (a,b,c): Wrapped images of the correlation fringes in the spectral field for Zamzam, bottled drinking and distilled waters respectively. The rotation angle was $\theta = 0.2^\circ$ at wavelength $0.6328 \mu m$. The distance between the rough surface and the observation plane Z was 75 cm.

Figure.(11). Relation between the six discrete wavelengths across the visible spectrum and the phase in radian Φ given by the new theoretical formulae and the phase map for Zamzam, bottled drinking and distilled waters.

Table 1. Dispersion of Optical parameters at $\lambda = 550nm$ for three waters using Cauchy's dispersion equation and the new theoretical equation

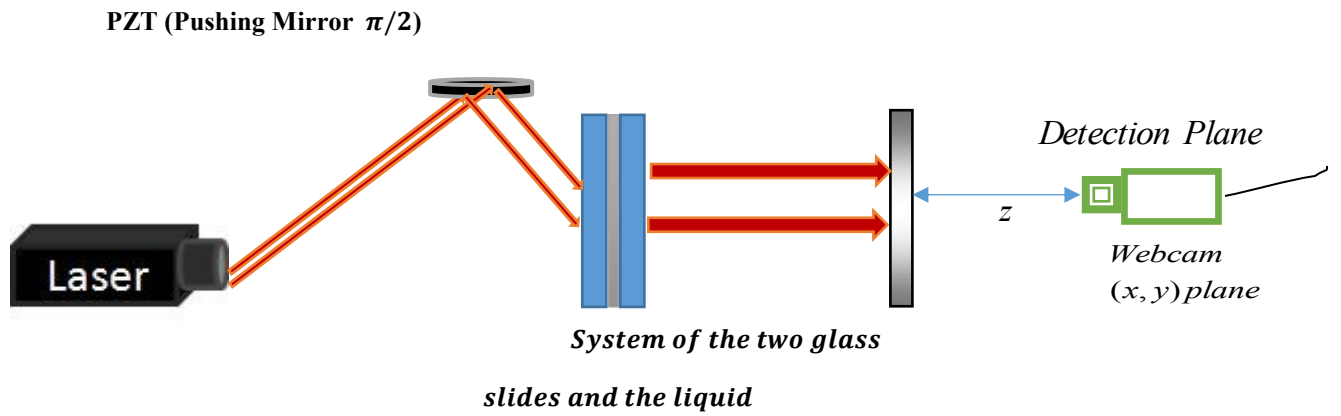


Fig.1.

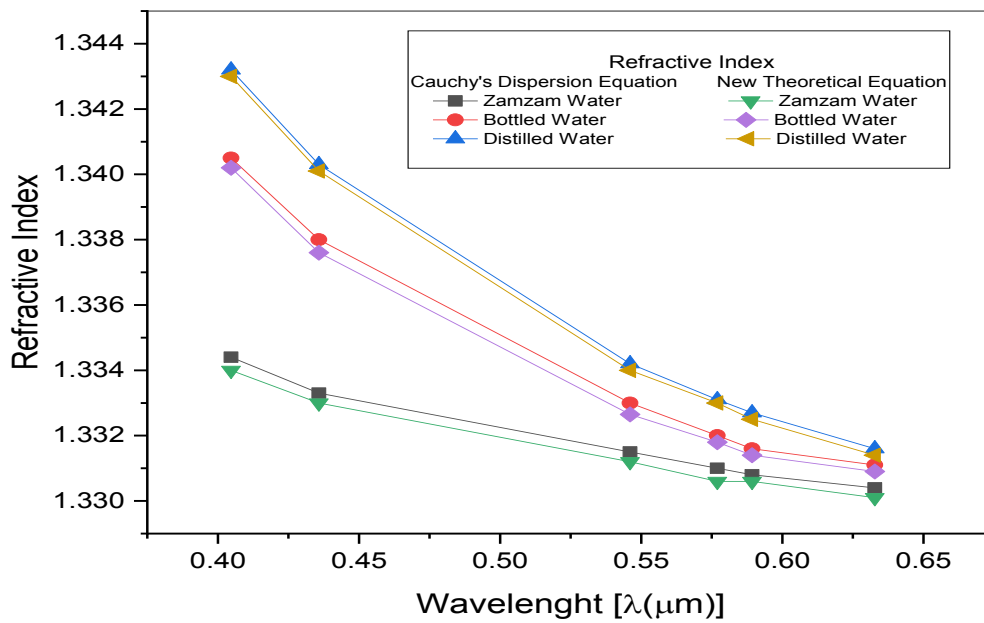


Fig.2.

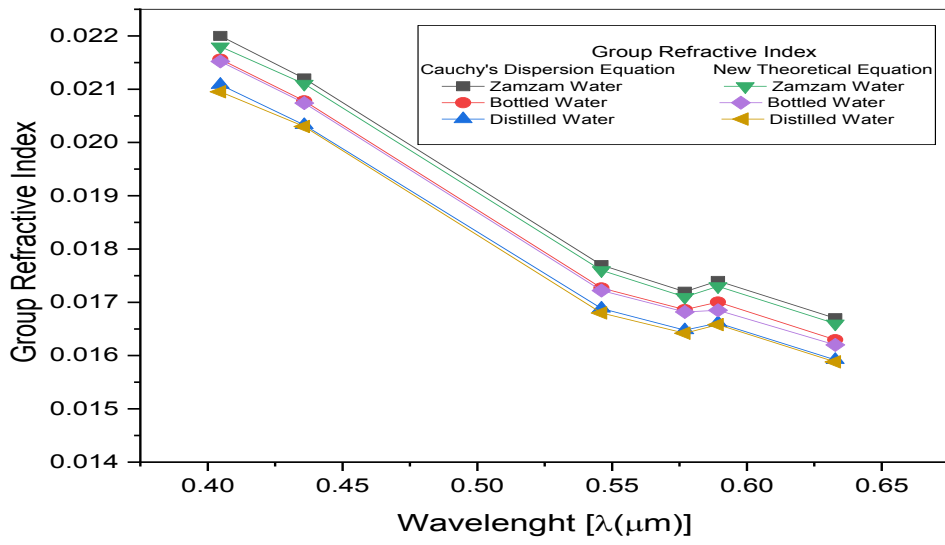


Fig.3.

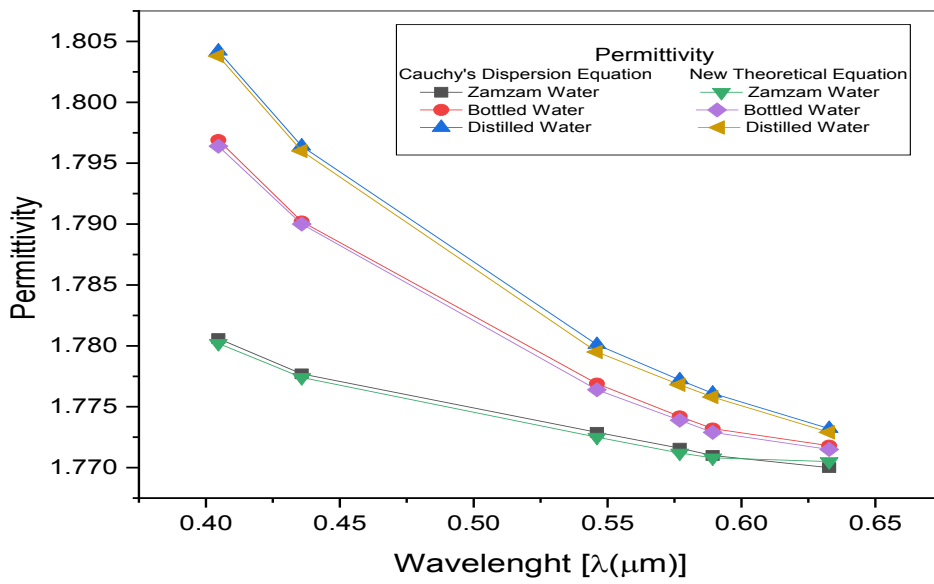


Fig.4.

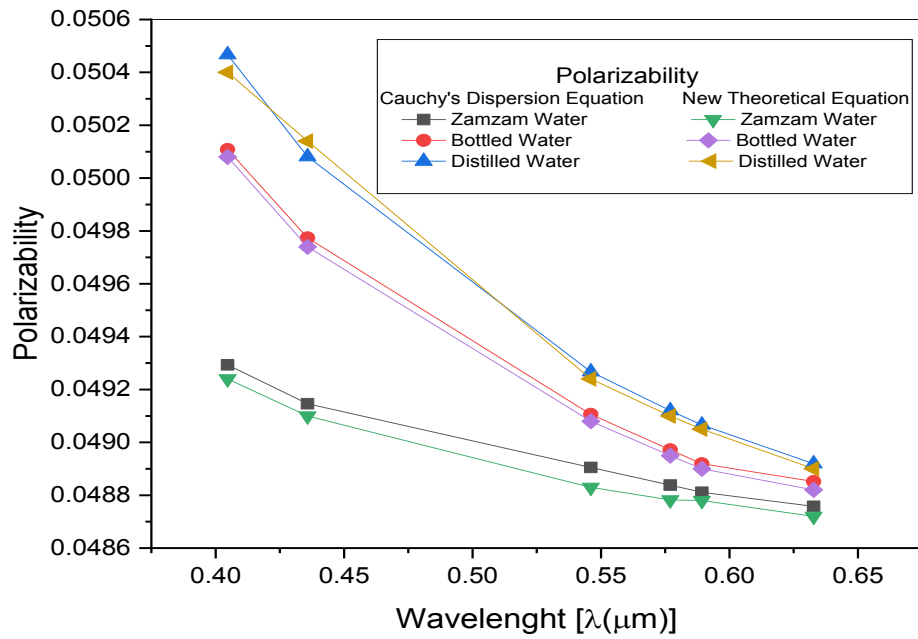


Fig.5.

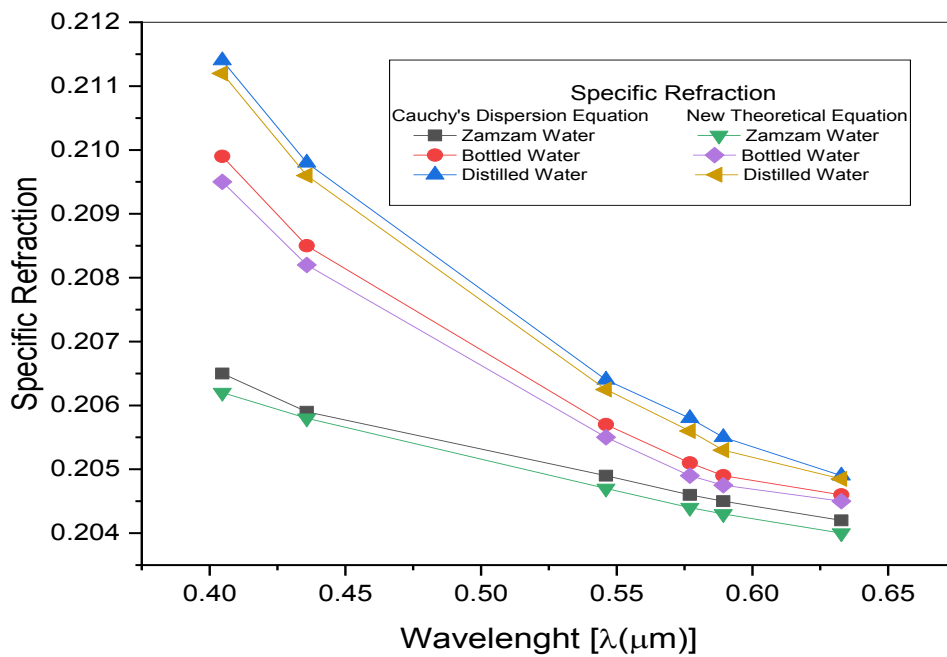


Fig.6.

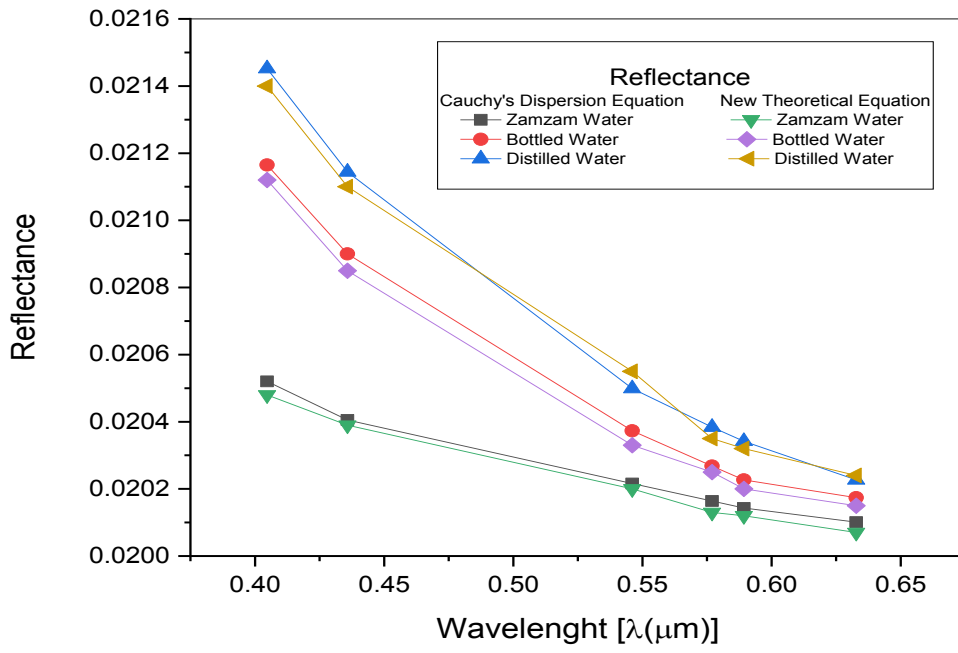


Fig.7.

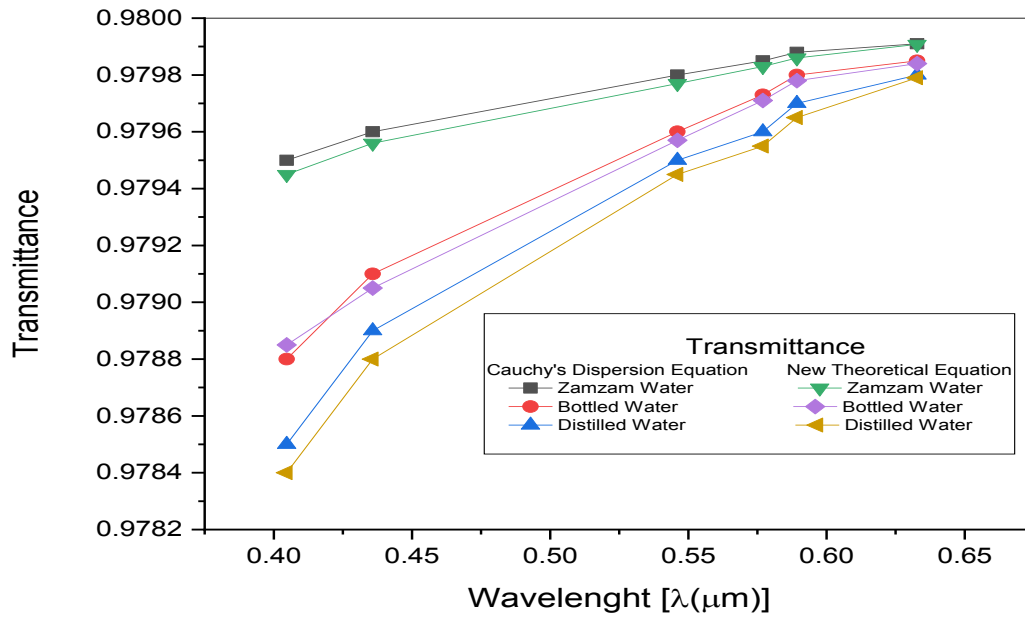


Fig.8.

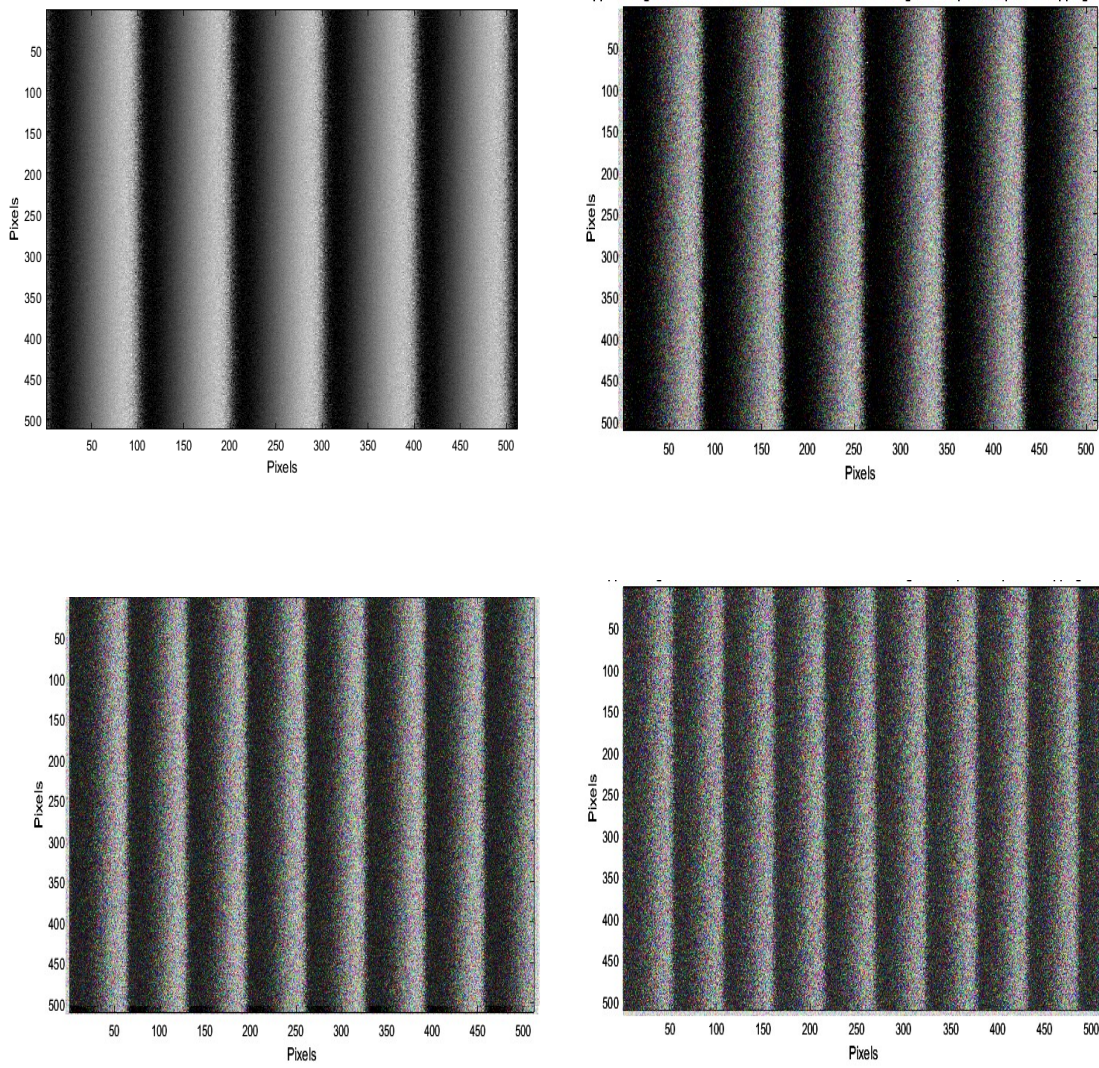
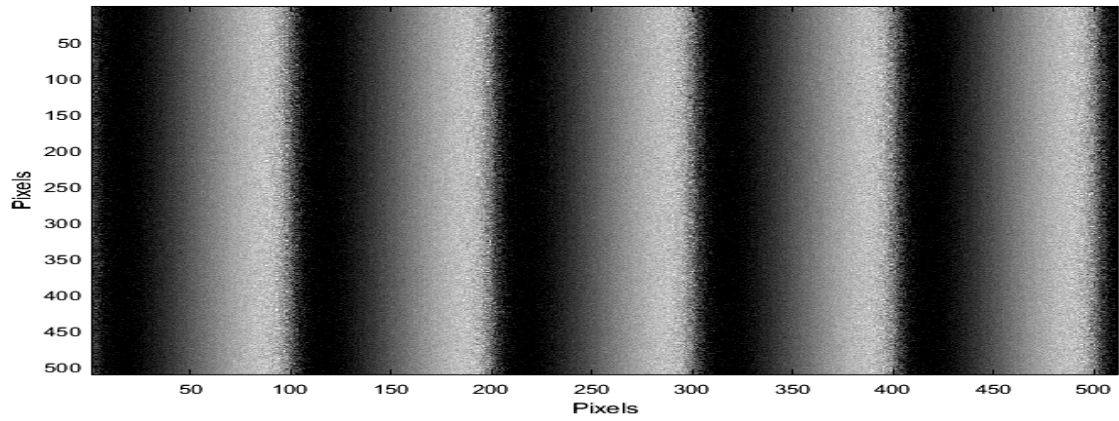
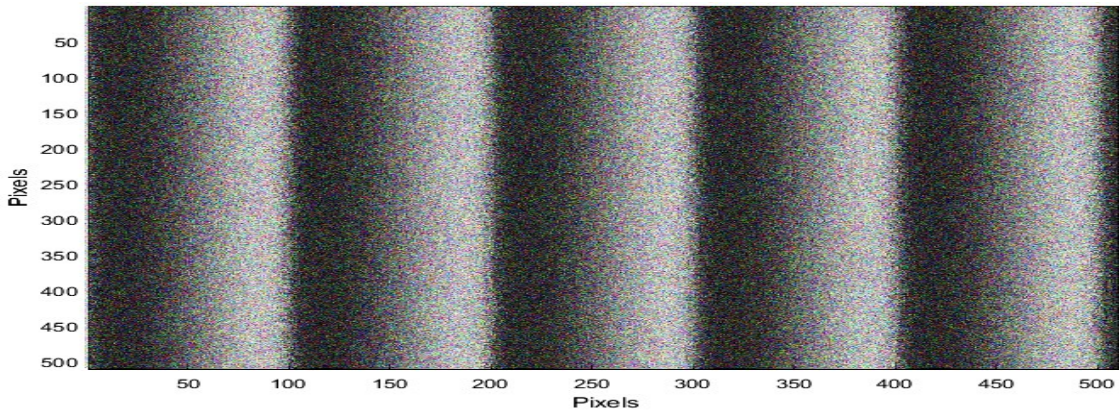


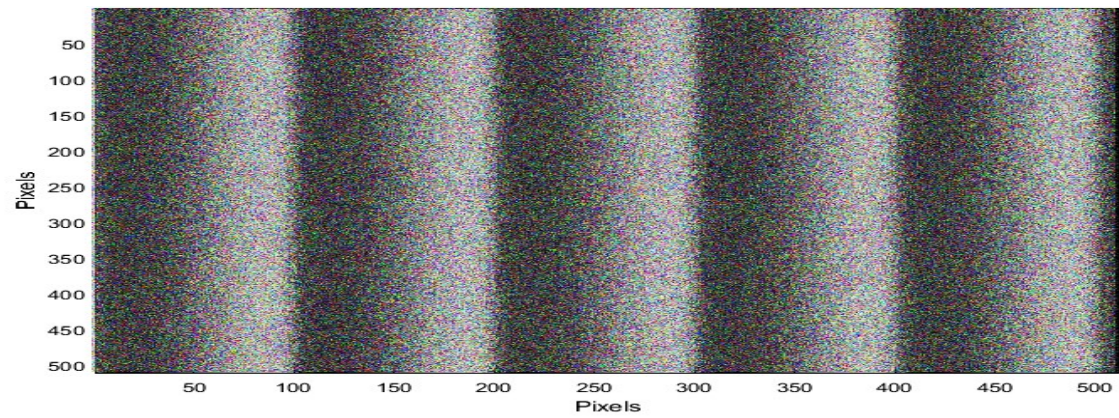
Fig. 9 (a,b,c,d)



(a)



(b)



(c)

Fig. 10 (a, b, c):

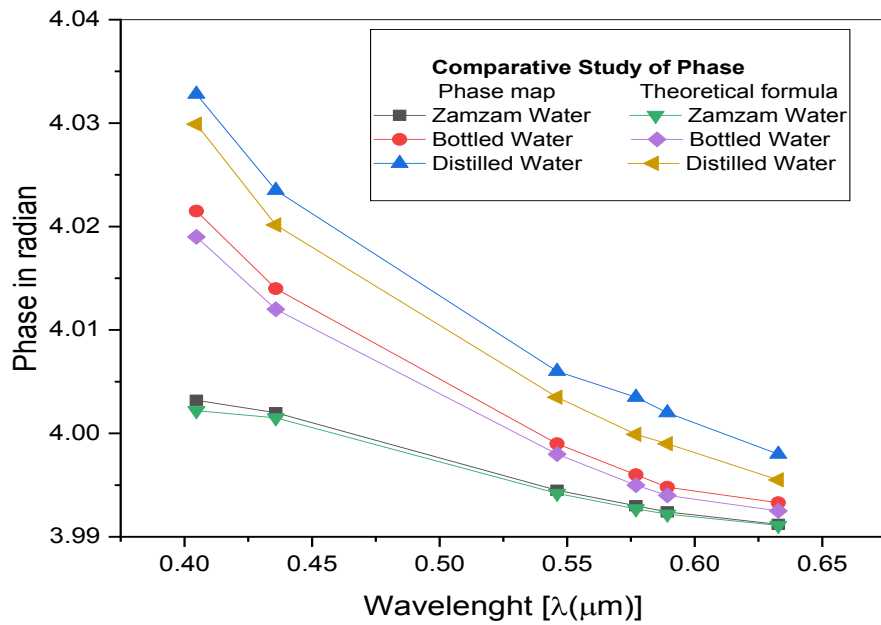


Fig.11.

Table 1.

Parameter	Dispersion for Zamzam water		Dispersion for Bottled water		Dispersion for Distilled water	
	Cauchy's Dispersion Equation	New Theoretical Equation	Cauchy's Dispersion Equation	New Theoretical Equation	Cauchy's Dispersion Equation	New Theoretical Equation
Refractive index	-1.2954×10^{-5}	-1.301×10^{-5}	-3.2954×10^{-5}	-3.3864×10^{-5}	-3.8637×10^{-5}	-2.9921×10^{-5}
Group refractive index	-3.8863×10^{-5}	-3.911×10^{-5}	-9.5721×10^{-5}	-8.988×10^{-5}	-1.1591×10^{-4}	-1.2102×10^{-4}
Permittivity	-3.4492×10^{-5}	-3.4534×10^{-5}	-8.5059×10^{-5}	-8.765×10^{-5}	-1.0309×10^{-4}	-1.1132×10^{-4}
Specific refraction	-3.6573×10^{-5}	-3.5321×10^{-5}	-9.0089×10^{-5}	-9.5643×10^{-5}	-1.091×10^{-4}	-0.9987×10^{-4}
Polarizability	-8.7312×10^{-6}	-9.3451×10^{-6}	-2.1507×10^{-5}	-1.9876×10^{-5}	-2.6045×10^{-5}	-2.3245×10^{-5}
Reflectance	-1.3549×10^{-6}	-1.4560×10^{-6}	-3.3464×10^{-6}	-3.5678×10^{-6}	-4.0605×10^{-6}	-3.9876×10^{-6}
Transmittance	3.1587×10^{-6}	3.2543×10^{-6}	7.807×10^{-6}	8.101×10^{-6}	9.4776×10^{-6}	9.5678×10^{-6}